

NAS 8-21432 D7
Reprinted from
Journal of Terramechanics, 1971, vol. 8, no. 1, pp. 59 to 69. Pergamon Press
Printed in Great Britain.

PENETRATION RESISTANCE OF LUNAR SOILS

W. N. HOUSTON* and L. I. NAMIQ†

INTRODUCTION

PENETRATION resistance tests are likely to be an efficient and effective means by



PERGAMON PRESS
OXFORD NEW YORK LONDON PARIS

PENETRATION RESISTANCE OF LUNAR SOILS

W. N. HOUSTON* and L. I. NAMIQ†

INTRODUCTION

PENETRATION resistance tests are likely to be an efficient and effective means by which astronauts may gather data leading to the assessment of lunar surface soil properties. Such tests are planned for future Apollo missions.

An important application of penetration resistance data may be in the trafficability analyses needed for range prediction for lunar roving vehicles. It is also anticipated that penetration resistance can be correlated with density for the lunar soil. In addition, abrupt changes in the slope of the stress-penetration curve may be used as indicators of nonhomogeneities in the soil profile.

USE OF LUNAR SOIL SIMULANT

A solution to the problem of determining the penetration resistance of lunar soils was obtained by selecting and testing a lunar soil simulant and then translating the relationships obtained to the lunar surface. The selection and subsequent modification of the simulant were based primarily on the following data:

- (a) Composition—Surveyor and Apollo 11 data indicated that basalt most closely represents lunar soil.
- (b) Gradation curves and cohesion values from Surveyor studies and Apollo 11 samples.
- (c) Penetration resistance of returned Apollo 11 material.

The well-graded silty sand shown in Fig. 1 was selected as the soil providing the best match for lunar soil. Gradation curves for Apollo 11 and 12 material are shown for comparison. The simulant was prepared by mixing crushed basalt powder with basalt sand. The penetration resistance of the simulant using a $\frac{1}{4}$ -in.-dia. rod penetrometer was measured in terms of the slope of the stress-penetration curve, G , for various densities. The relationship obtained is compared in Fig. 2 with a limited amount of similar data obtained on earth-returned samples of Apollo

*Assistant Professor of Civil Engineering, University of California, Berkeley, California, U.S.A.

†Graduate Research Assistant, University of California, Berkeley, California, U.S.A.
Communicated by I. R. Ehrlich.

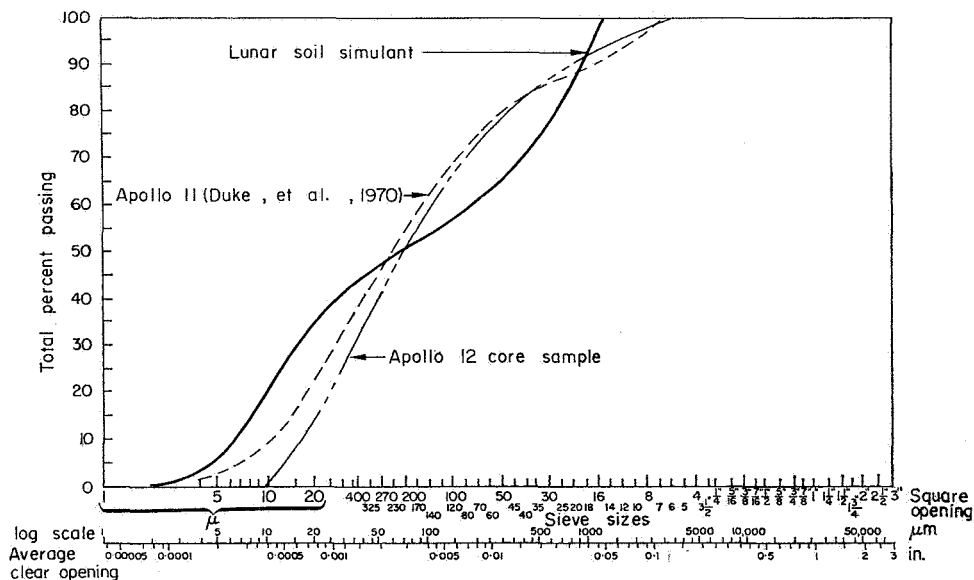
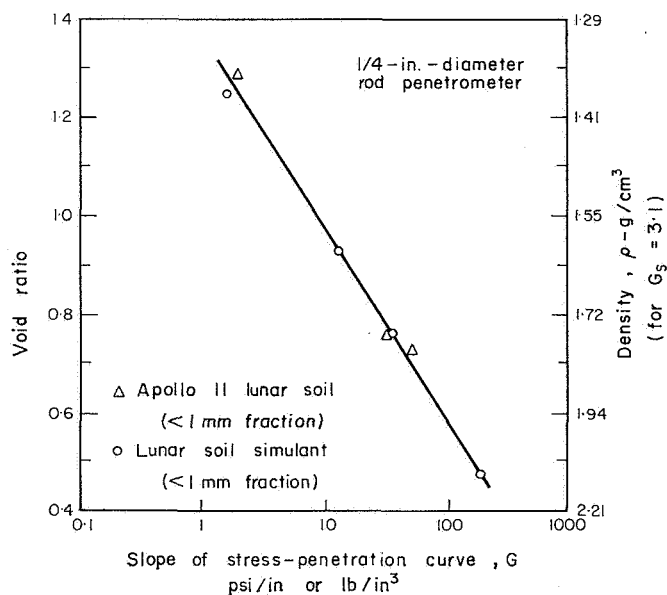


FIG. 1. Gradation curves for lunar soil simulant and Apollo 11 and 12 material.

FIG. 2. Relationship between G and void ratio for Apollo 11 lunar soil and for lunar soil simulant.

11 material. The comparison indicates that the simulant is a good match for the lunar soil, at least in regard to penetration resistance behavior.

Cohesion comparable to that of the lunar soil was obtained in the simulant by maintaining a small moisture content of about 2 per cent.

PENETRATION RESISTANCE OF SIMULANT

Although penetration resistance of the simulant had been obtained for the $\frac{1}{4}$ -in.-dia. rod, additional tests with a more widely used penetrometer were considered desirable. Also, the $\frac{1}{4}$ -in.-dia. rods were inserted to a depth of only 1–2 in., and greater depths are of interest. The cone penetrometer chosen for additional testing has the cone configuration of the Waterways Experiment Station penetrometer shown in Fig. 3. Various devices may be used to measure load; a proving ring

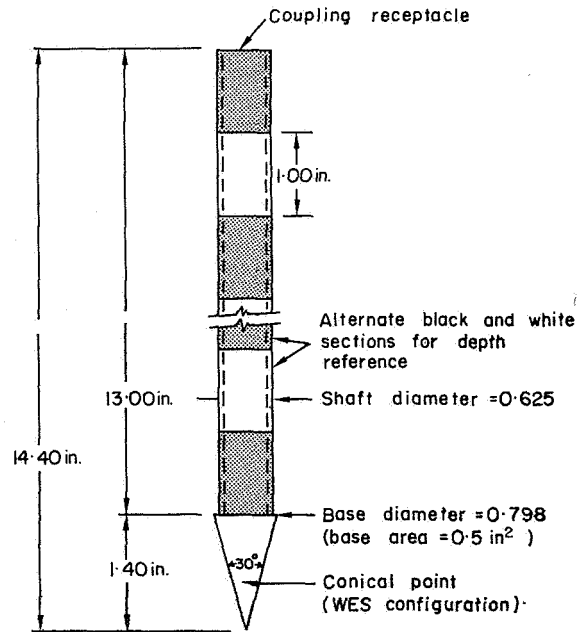


FIG. 3. Penetrometer cone and shaft.

was used in this study. Alternate black and white one-inch sections were marked on the shaft to provide a visual measure of the depth of penetration.

An example stress-penetration curve is shown in Fig. 4. The position of the feet of the man performing the test with respect to the penetrometer has an effect on the results. Therefore, the position indicated in the upper left corner of Fig. 4 was adopted as standard. The penetrometer was advanced at the rate of about 1 in. per 5 sec to avoid the development of pore air pressures; however, a penetrometer on the lunar surface could be advanced at a greater rate.

A series of penetration resistance tests was performed on the simulant using the cone penetrometer. The slope of the stress-penetration curve, G , is plotted vs. the average void ratio for the top 15 cm in Fig. 5. One of the uses of the data in Fig. 5, in connection with trafficability studies, is that of comparing the G vs. e_{avo} relationship of any new proposed lunar soil simulant to that in Fig. 5. Because available data indicate this simulant is a good match for the actual lunar soil, Fig. 5 can be used as an indicator of the suitability of any new soil that might be used for LRV simulation studies.

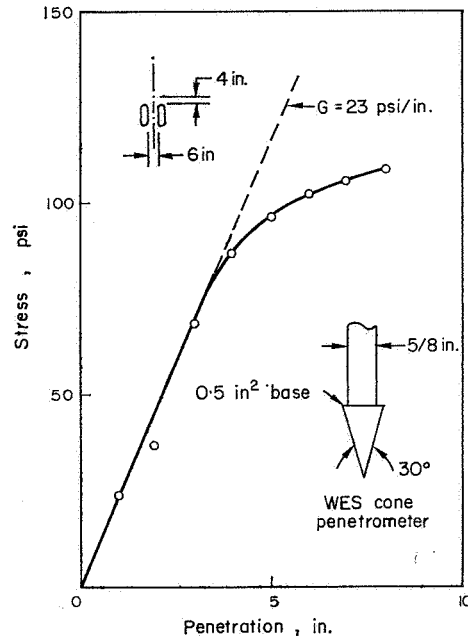
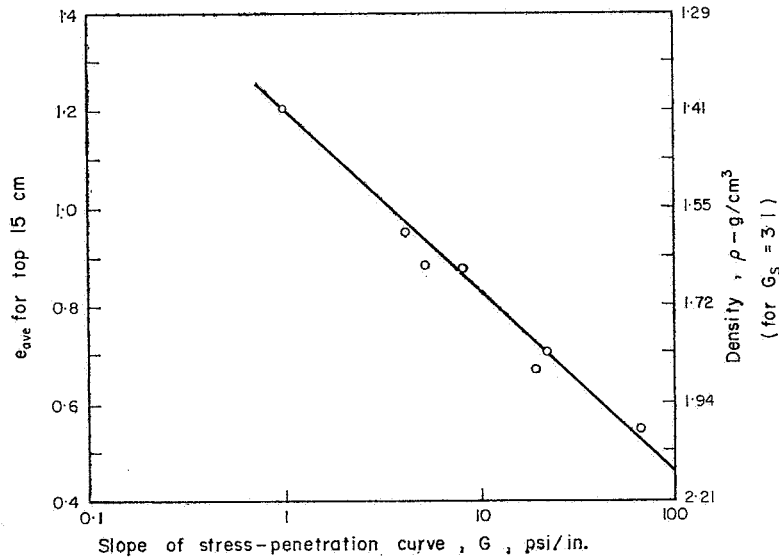


FIG. 4. Example stress-penetration curve.

FIG. 5. Relationship between G and void ratio for simulant under full gravity.

PENETRATION RESISTANCE OF LUNAR SOIL

Figure 5 provides the relationship between G and e_{ave} for terrestrial gravity. An estimate of the variation of G with e_{ave} for lunar gravity was obtained by applying the following bearing capacity equation to the penetrometer:

$$q_{ult} = \frac{b\gamma}{2} N_\gamma s_\gamma + c N_c s_c + q' N_q s_q, \quad (1)$$

where q_{ult} = unit ultimate bearing capacity
 γ = soil unit weight
 b = width of loaded area
 c = soil cohesion
 q' = surcharge, $d\gamma$
 s_γ = shape factor $(1 - 0.3 b/L)$
 s_c = shape factor $(1 + 0.2 b/L)$
 s_q = shape factor $(1 + 0.2 b/L)$
 N_γ, N_c, N_q = bearing capacity factors, dependent on the soil friction angle, ϕ
 d = depth of loaded area
 L = length of loaded area.

The penetrometer has a diameter of about 0.8 in. which was used for b . A value of $b/L=1$ was used for all computations.

The needed soil strength parameters, c and ϕ , were determined by laboratory tests on the simulant. Both parameters were found to vary with soil density as shown by Figs. 6 and 7. The friction angle, ϕ , was also found to vary with confining

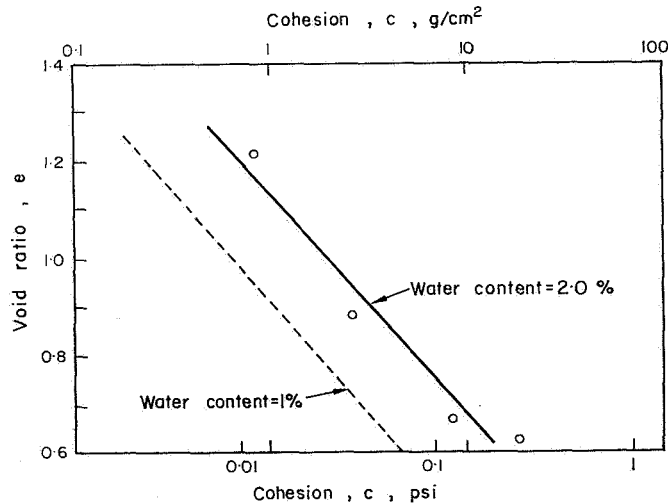


FIG. 6. Relationship between cohesion, c , and void ratio, e , for simulant.

pressure, but the data in Fig. 7 represent average values.

The density of lunar soil is expected to vary with depth and this variation would influence penetration resistance. It was assumed that lunar soil deposits were formed by the deposition of a thin surficial layer at some initial density followed by densification due to the weight of overlying layers deposited subsequently. The degree of densification to be expected from compression by overlying layers was estimated by measuring the compressibility of the simulant in one-dimensional compression tests. Compressibilities of specimens placed at various initial densities were used to develop a family of density vs. depth curves for the simulant, as shown in Fig. 8. These curves were verified experimentally by measuring densities at

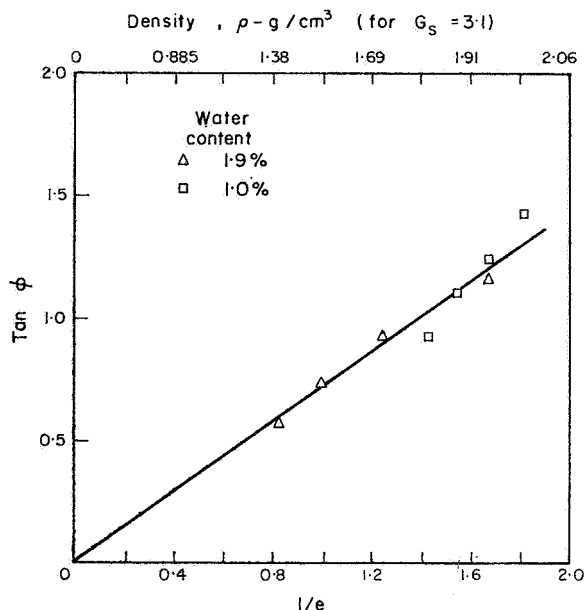
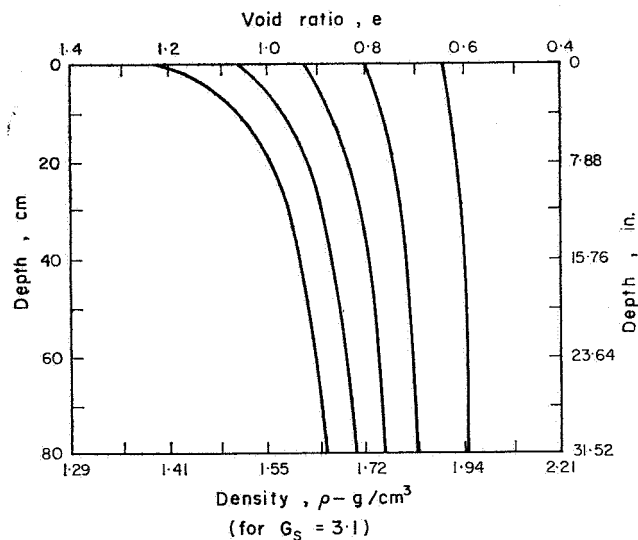
FIG. 7. Relationship between ϕ and void ratio for simulant.

FIG. 8. Variation of void ratio with depth for simulant with terrestrial gravity.

various depths in typical deposits of the simulant. Note that the density at depths as great as 30 in. depends strongly on the initial density at the surface. A similar family of curves was developed for the lunar surface by using the same compressibility parameters but smaller gravity stresses consistent with lunar gravity. Fig. 9 shows the predicted density profiles for the lunar surface. Note that reduced gravity results in a less pronounced increase in density with depth.

For the first set of computations a soil profile consistent with terrestrial gravity was chosen from Fig. 8. The bearing capacity was computed for a depth, d , equal to 0 and 15 cm. The void ratio for $d=0$ and $d=15$ cm were taken from Fig. 8 and used to enter Figs. 6 and 7 to obtain values for c and ϕ . Meyerhof's charts [1] were used for the bearing capacity factors.

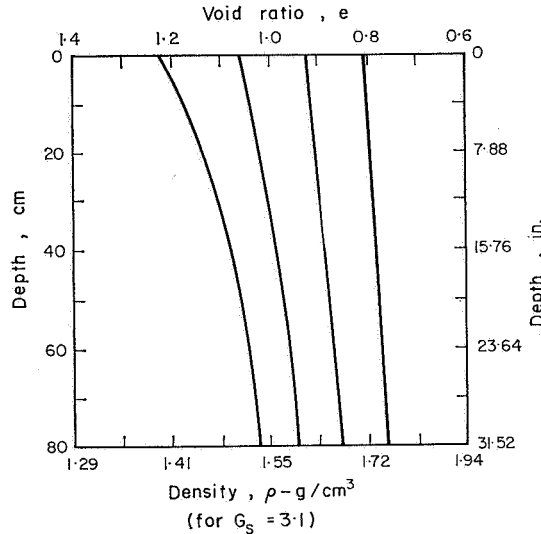


FIG. 9. Predicted variation of void ratio with depth for actual lunar soil under lunar gravity.

For a compressible soil that may experience local shear, the bearing capacity is usually computed by using reduced strength parameters c_r and ϕ_r , so that

$$c_r = k_{ls} c \quad (2)$$

$$\phi_r = \arctan (k_{ls} \tan \phi). \quad (3)$$

The value of k_{ls} varies from 1 to 0.67, depending on soil compressibility. A value close to 0.67 is indicated for the simulant because no bulging was observed around the penetrometer during testing. A value of $k_{ls}=0.75$ was used for all computations.

The stress-penetration gradient, G , was taken as the change in q_{ult} between $d=0$ and $d=15$ cm divided by 15 cm. Values of G obtained in this way were plotted vs. e_{ave} for the top 15 cm.

The results are shown in Fig. 10, where measured and computed values are compared. The close agreement indicates that the bearing capacity equation provides a reasonable basis for estimating G values. Accordingly, the same relationship was used to investigate the probable influence of gravity on G value.

The bearing capacity computations were repeated for reduced gravity using the same factors, except that $\gamma/6$ was used instead of γ for the density. A void ratio-depth profile more consistent with the lunar surface (as given in Fig. 9) was used.

The G values obtained in this way were used to determine the ratio, R_p , of G

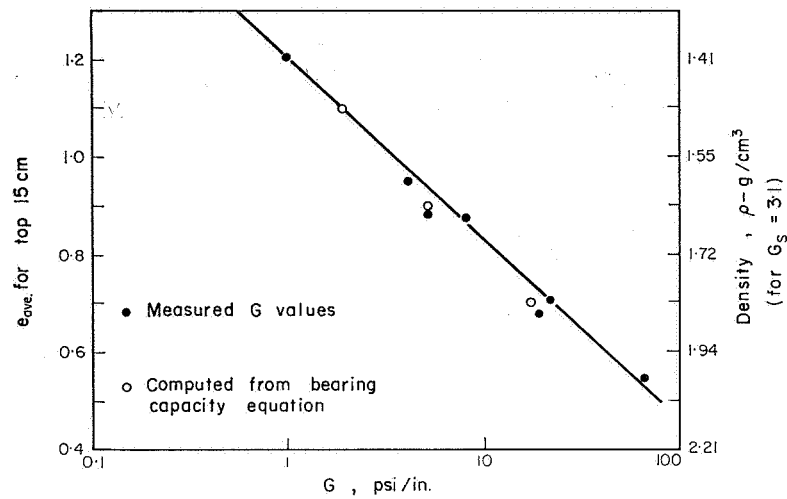


FIG. 10. Comparison of measured and computed G values for simulant under full gravity.

under lunar gravity to G under terrestrial gravity with the result shown in Fig. 11. A value of $R_p = 1$ corresponds to no reduction in G value due to reduced gravity of the lunar surface. A value of $R_p = 0.167$ corresponds to a reduction in G which is in direct proportion to terrestrial and lunar gravity; i.e. 1:6. Figure 11 shows

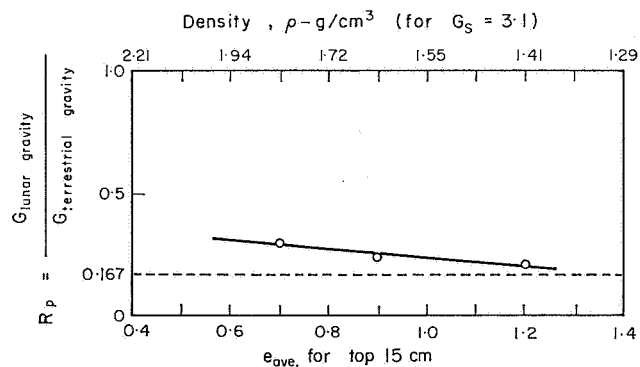
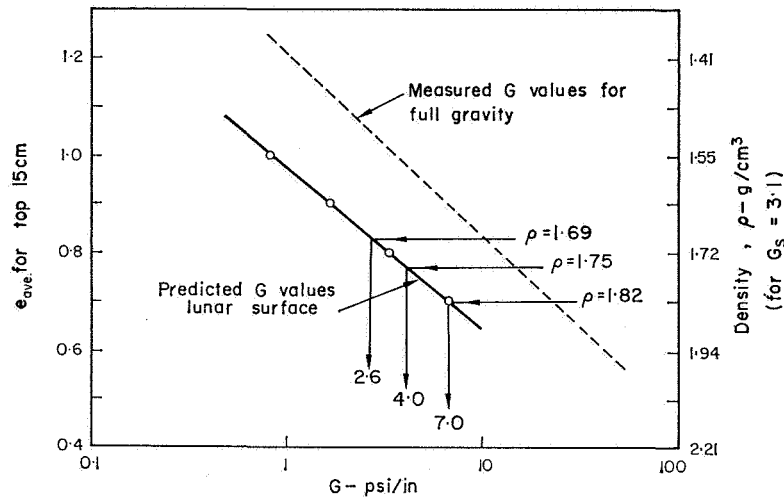


FIG. 11. Variation of G value reduction factor, R_p , with void ratio.

that the R_p values developed in this investigation fall between these two extremes, with an average value of about 0.25. This means that if a lunar soil profile yielded a G value of 2 psi/in. on the lunar surface, a terrestrial soil profile with the same average density would be expected to yield a G value of about 8 psi/in.

Reduction factors from Fig. 11 were applied to the measured terrestrial G values (shown by the lines in Figs. 5 and 10) to obtain the predicted G values for the lunar surface shown in Fig. 12.

FIG. 12. Predicted variation of G value with void ratio for actual lunar surface

From independent studies of astronaut footprint depths [2], which were made using the finite element method of analysis, it was determined that a reasonable range in the lunar soil density for the top 15 cm is about 1.69 to 1.82 g/cm³, with an expected average value of about 1.75 g/cm³. This range in density is consistent with density values obtained from Apollo 12 core tubes. The corresponding range in predicted G values from Fig. 12 is summarized in Table 1.

TABLE 1. SUMMARY OF PREDICTED G -VALUES FOR LUNAR SURFACE

	Density, ρ (g/cm ³) (for top 15 cm, using $G_s = 3.1$)	Penetration resistance gradient, G (psi/in)
Expected average value	1.75	4.0
Upper limit	1.82	7.0
Lower limit	1.69	2.6

CONCLUSIONS

1. The bearing capacity equation (1) provides a reasonable basis for estimating penetration resistance gradient, G , if local shear strength parameters are used and increase in density and shear strength with depth is accounted for.
2. The rate of increase in density and shear strength with depth influences the penetration resistance gradient, G . The density increase with depth is expected to be more pronounced on earth than for the same soil on the moon—due to lower gravity stresses on the lunar surface.
3. The factor by which the penetration resistance is reduced due to lunar gravity is less than the factor 6, which relates terrestrial and lunar gravity. An average factor of about 4 (corresponding to $R_p = 1/4$) was found in this study.

4. Using current estimates of lunar soil density, the relationships developed in this study indicate a range in G value of about 2.6 to 7 psi/in, with an expected average value of about 4 psi/in.
5. If improved estimates of lunar soil density subsequently become available, Fig. 12 may be used to estimate G values in the absence of a more direct correlation.
6. The stress penetration gradient, G , is a sensitive measure of density and Fig. 12 may also be entered with measured values of G to obtain estimates of density.
7. Stress penetration gradients may be used to indicate non-homogeneities in the soil profile, as shown by Fig. 13.

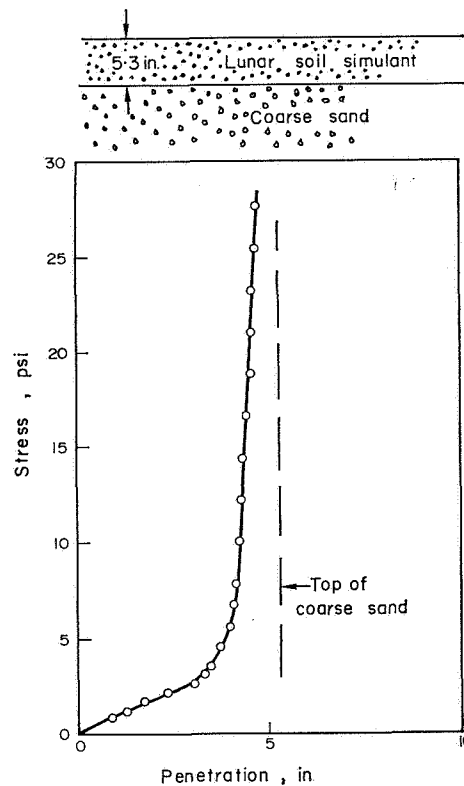


FIG. 13. Stress-penetration curve for two-layer profile.

NOTATION

- b width of loaded area
 c cohesion, g/cm² or lb/in²
 c_r reduced cohesion value, g/cm² or lb/in²
 d depth of loaded area
 e void ratio
 e_{ave} average void ratio for top 15 cm
 G slope of stress-penetration curve, psi/in., for cone penetrometer tests
 G_s specific gravity
 k_{ls} reduction factor
 L length of loaded area

N_γ, N_c, N_q	bearing capacity factors
q_{ult}	unit ultimate bearing capacity, g/cm ² or lb/in ²
R_p	penetrometer G -value reduction factor for reduced gravity
s_γ, s_c, s_q	shape factors for bearing capacity equations
WES	Waterways Experiment Station
γ	soil unit weight, g/cm ³
ϕ	friction angle, degrees
ϕ_r	reduced friction angle, degrees
ρ	density, g/cm ³

Acknowledgements—The data used in the preparation of this paper was obtained under Contract Number NAS 8-21432 with the George C. Marshall Space Flight Center of the National Aeronautics and Space Administration. The work was administered under the technical direction of the Space Sciences Laboratory of the George C. Marshall Space Flight Center.

REFERENCES

- [1] G. G. MEYERHOF. *The Ultimate bearing Capacity of Foundations*, Vol. II, p. 301, Geotechnique (1951).
- [2] L. I. NAMIQ. Stress-deformation study of a simulated lunar soil. Dissertation presented to the University of California, Berkeley, in 1970, in partial fulfilment of the requirements for the degree of Doctor of Philosophy.